NATIONAL ADVISORY COMMITTEE FOR AERONAUTICS

TECHNICAL NOTE 3232

AN ANALYSIS OF THE STABILITY AND ULTIMATE BENDING STRENGTH OF MULTIWEB BEAMS WITH FORMED-CHANNEL WEBS

By Joseph W. Semonian and Roger A. Anderson

Langley Aeronautical Laboratory
Langley Field, Va.

Washington
August 1954

NATIONAL ADVISORY COMMITTEE FOR AERONAUTICS

TECHNICAL NOTE 3232

AN ANALYSIS OF THE STABILITY AND ULTIMATE BENDING STRENGTH OF MULTIWEB BEAMS WITH FORMED-CHANNEL WEBS

By Joseph W. Semonian and Roger A. Anderson

SUMMARY

Design curves and procedures are presented for calculating the stresses for instability and failure of multiweb beams with formed-channel webs. The ultimate bending strength of this type of construction is shown to depend upon the deflectional stiffness of the web attachment flanges. A simple criterion is also given for predicting whether a multiweb beam with a given attachment-flange design will be susceptible to a wrinkling instability or will buckle as if the webs were integrally joined to the cover skins.

The criteria for predicting buckling and failure stresses are compared with experimental data. These criteria are sensitive to the offset, pitch, and diameter of the rivets used on the web attachment flanges, and the riveting specification is, therefore, emphasized as an important design consideration.

INTRODUCTION

Experiments have shown the existence of two distinct modes of instability and failure for multiweb beams subjected to bending loads. One mode, referred to herein as local buckling, is characterized by longitudinal nodes along the joints between webs and cover skins. The other mode is evidenced by a buckle pattern with troughs and crests extending across the entire width of the beam and without formation of longitudinal nodes. This mode is referred to herein as wrinkling, by analogy to a form of instability which may occur in the face plates of compressed sandwich panels.

In reference 1, design information for multiweb beams is presented, which is based on the assumption that the beam webs possess enough deflectional stiffness to enforce longitudinal nodes in the compressive cover skin when it buckles. In the tests of multiweb beams reported in reference 2, it was observed that, when local buckling occurred, the

buckling stresses correlated with the theory of reference 1. However, for beams of this series with formed-channel webs, wrinkling instability and failure were obtained. These tests, as well as the extensive experimental investigation of multiweb beams with formed-channel webs reported in reference 3, showed that, for a range of beam proportions, wrinkling instability and failure can occur at stresses far below those predicted by the local-buckling theory of reference 1.

The first published theoretical analysis of wrinkling behavior in multiweb beams was given in reference 4. The appraisal and application of this analysis, however, are handicapped by the lengthy procedure involved in calculating the buckling and failure stresses.

The purpose of the present paper is to develop a simple method of calculating both the stress at which initial wrinkling occurs in multiweb beams and the ultimate bending strength of beams which are susceptible to this mode of instability. The method makes use of an expression for the deflectional stiffness of formed-channel webs, derived herein, and the stability criteria of reference 5, which relate the cover-plate buckling-stress coefficient to the effective deflectional stiffness of the supporting members. The calculation of the ultimate bending strength is based upon the concept, suggested in reference 2, that the beam cover may be treated as a wide column supported upon an elastic foundation.

The analytical results are compared with the extensive test data of reference 3. Detailed analytical derivations are confined to the appendixes of the paper.

SYMBOLS

b_s width of cover skin between rivet lines of webs

b_w web depth measured between center lines of attachment flanges

D_f flange flexural stiffness per unit width, $\frac{Et_f^3}{12(1-\mu^2)}$

D_s cover-skin flexural stiffness per unit width, $\frac{Et_s^3}{12(1-\mu^2)}$

D_w web flexural stiffness per unit width, $\frac{Et_w^3}{12(1-\mu^2)}$

E Young's modulus of elasticity

E_{sec} secant modulus of elasticity

E_{tan} tangent modulus of elasticity

f distance between web plane and a line along which rivets effectively clamp attachment flange to cover skins

g amplitude of sinusoidally distributed lateral load

k_c failure-stress coefficient

k_s buckling-stress coefficient for cover skin

N compressive load per unit width acting in x-direction

t_f thickness of attachment flange

t_s thickness of cover skin

t_w web thickness

x, y coordinate axes in length and width directions, respectively

α rotational stiffness per unit length of web (moment per unit length required to produce rotation of 1 radian)

$\beta = \frac{\lambda}{f}$

η plasticity coefficient for beam in failure mode, $\sqrt{\eta_s \eta_w}$

η_s plasticity coefficient for cover skin

η_w plasticity coefficient for web

$\theta = \pi \frac{b_s}{\lambda} \sqrt{\frac{\lambda}{b_s} \sqrt{k_s} + 1}$

λ half wave length of sinusoidal deflection; also, buckle length

μ Poisson's ratio

σ_c failure stress for cover skin determined from column analysis

σ_{cr} buckling or wrinkling stress

$$\varphi = \pi \frac{b_S}{\lambda} \sqrt{\frac{\lambda}{b_S} \sqrt{k_S} - 1}$$

ψ deflectional stiffness per unit length of support

ψ_1, ψ_2 measured deflectional stiffnesses per unit length of web

ψ' substitute deflectional stiffness per unit length of support

$\frac{\alpha b_W}{D_W}$ nondimensional rotational restraint parameter

$\frac{\psi b_S^3}{\pi^4 D_S}$ nondimensional deflectional restraint parameter

STRUCTURAL ANALYSIS

The present analysis of multiweb beams is based upon an idealization of the compression skin as a plate restrained against deflection by elastic-line supports of equal stiffness. The structural idealization is illustrated in figure 1, where the web members are shown replaced by elastic supports which have a deflectional stiffness ψ per unit length of support.

The analysis is divided into three sections. The first section is devoted to initial instability in the wrinkling mode. The concepts developed in the first section are verified experimentally in the second section, whereas in the third section these concepts are used to develop a criterion for the ultimate bending strength of multiweb beams.

Initial Instability

The wrinkling mode of instability, as it can occur in multiweb beams, is shown in figure 2. In this form of instability, longitudinal nodes are not formed, and the buckle deflection extends across the entire width of the beam with only slight decreases in amplitude at the spanwise web joints.

In reference 5, the following stability criterion was derived in terms of ψ, the deflectional stiffness per unit length of support:

$$\frac{\psi b_S^3}{\pi^4 D_S} = \frac{\dfrac{4\sqrt{k_S}}{\pi^2 \dfrac{\lambda}{b_S}}}{\dfrac{\dfrac{\sin \varphi}{\varphi}}{1 - \cos \varphi} - \dfrac{\dfrac{\sinh \theta}{\theta}}{1 - \cosh \theta}} \tag{1}$$

The nondimensional deflectional restraint parameter $\frac{\psi b_S^3}{\pi^4 D_S}$ is a measure of the resistance with which the supporting members (in the present case, the formed-channel webs) oppose deflection of the compression cover of the beam. In order to apply this criterion to an actual structure, the deflectional restraint parameter must be evaluated for the supporting members of that structure.

By assuming that the web attachment flanges act as cantilever-type connections between the webs and cover skins, the following expression for the resistance with which a formed-channel web opposes cover deflection is derived in appendix A:

$$\frac{\psi b_S^3}{\pi^4 D_S} = \frac{\dfrac{12}{\pi^4}}{\left(\dfrac{b_W/t_W}{b_S/t_S}\right)^3 \left(\dfrac{f}{b_W}\right)^3} \frac{\dfrac{f}{b_W}\dfrac{\alpha b_W}{D_W} + 1}{\dfrac{f}{b_W}\dfrac{\alpha b_W}{D_W} + 4} \tag{2}$$

In this equation, the deflectional restraint parameter $\frac{\psi b_S^3}{\pi^4 D_S}$ is given in terms of the structural dimensions of the beam and the effective rivet offset distance f. The effective rivet offset distance, or, more briefly, the f-distance, is defined as the distance from the web plane to the line along which the rivets effectively clamp the attachment flange to the cover skin. It is seen from equation (2) that the capacity of a formed-channel web to resist cover buckling is largely determined by the f-distance. In addition to being a function of the actual offset distance of the rivet center line, the f-distance is influenced by all the factors which affect the clamping of the attachment flange to the cover skin, such as rivet pitch, diameter, and head dimensions. The parameter $\frac{\alpha b_W}{D_W}$ in equation (2) is a measure of the rotational-edge restraint which the web of the channel offers the flange and is a function

of the web stress and the wave length of buckling. It is numerically equal but opposite in sign to the quantity ϵ in reference 1 and may be evaluated from figure 9 of that paper.

Equations (1) and (2) may be solved simultaneously to obtain the buckling-stress coefficient for the wrinkling mode k_S in terms of the beam dimensions. Such calculations have been made and the results are presented as buckling curves in figure 3. Although the two ratios $\frac{f}{b_W}$ and $\frac{b_W/t_W}{b_S/t_S}$ used for the buckling curves are not sufficient to determine beam proportions, calculations indicated that they are sufficient to determine the value of the buckling coefficient.

When the curves from reference 1 for the local buckling-stress coefficients are plotted against the parameter $\frac{b_W/t_W}{b_S/t_S}$, they lie so close together for most of the design range that, for purposes of comparison, they may be represented by a single curve, as in figure 3. This curve, then, defines the boundary between wrinkling and local buckling. From figure 3, it may be verified that, in order to avoid a wrinkling instability, the product $\frac{f}{b_W}\left(\frac{b_W/t_W}{b_S/t_S}\right)$ or, simply, $\frac{f}{t_W}\frac{t_S}{b_S}$ must be less than approximately 0.18. For values greater than about 0.18, wrinkling will be the governing mode of instability.

The sensitivity of the wrinkling-stress coefficient to the f-distance is evident from the curves of figure 3. In most beams, the f-distance is a fraction of an inch and, therefore, seemingly small changes in the rivet offset, pitch, and diameter can produce substantial percentage changes in $\frac{f}{b_W}$ and, thus, in beam wrinkling stress. For example, the effect of changes in the offset of the rivet line from the web plane, caused by changes in flange bend radius, has been illustrated by the tests reported in reference 6. Similarly, it appears that test data (of which ref. 7 is representative) on the influence of rivet pitch and diameter on the compressive strength of skin stringer panels also reflect the effect which changes in the effective rivet offset distance have on panel strength. An analysis of this extensive data from the standpoint of relating the effective rivet offset distance to the riveting specification for the flange would be desirable.

One approach to the evaluation of the f-distance for a given flange design is discussed in appendix B. This method is based upon experimentally measured values of flange stiffness obtained under a simple loading condition, and, at least for the beam proportions of reference 3, appears to

give satisfactory results. A comparison of the experimental data for multiweb beams with the buckling theory in terms of the f-distance concept is presented in the next section.

Experimental Verification of f-Distance Concept

The data of reference 3 were obtained in pure-bending tests of multiweb beams with channel-type webs which had been cold formed from 75S-T6 aluminum-alloy sheet 0.051 inch thick to bend radii of four times the web thickness. The tests are divided into three groups corresponding to ratios of web thickness to skin thickness $\frac{t_W}{t_S}$ of 0.27, 0.41, and 0.63. In each group, the attachment flange and rivet pattern used on the beams had the same design specifications; hence, a constant value of $\frac{f}{t_W}$ should apply to all beams with a given ratio $\frac{t_W}{t_S}$.

In the group of 20 beams with $\frac{t_W}{t_S} = 0.41$, a wrinkling instability was observed in 10 beams. These 10 beams had ratios of skin width to skin thickness $\frac{b_S}{t_S}$ of 25 and 30 and had ratios of channel-web depth to web thickness $\frac{b_W}{t_W}$ of 30, 40, 60, 80, and 120. Beams with $\frac{b_S}{t_S} = 40$ and 60 and $\frac{b_W}{t_W} = 30$, 40, 60, 80, and 120 were observed to buckle locally. All beams buckled in the elastic-stress range of the material.

Buckling-stress coefficients can be computed for the beams from the experimental buckling stresses by using the equation

$$k_S = \frac{\sigma_{cr} t_S b_S^2}{\pi^2 D_S} \tag{3}$$

A comparison of these experimental buckling-stress coefficients with wrinkling theory is shown in figure 4. The solid curves represent $\frac{f}{t_W} = 7$ $\left(f = 7t_W \text{ was experimentally determined for this flange design by the method of appendix B}\right)$. Correspondingly, the curves are labeled with values of $\frac{f}{b_W} = \frac{7}{30}, \frac{7}{40}$, and so forth. When the product $\frac{f}{b_W} \frac{b_W/t_W}{b_S/t_S}$

becomes greater than 0.18, the test data (solid symbols) follow the trend of the curves for the wrinkling theory. The open symbols, representing beams which buckled locally, appear to correlate with the theory of reference 1, represented by the dashed curve.

The agreement between experimental data and the curves of figure 4 indicates the validity of a stability analysis based upon the effective rivet offset distance of the web attachment flanges. In the next section, an extension of the analysis makes use of this concept of flange stiffness to establish a criterion for ultimate strength.

Failure Criterion

The experimental data of reference 3 show that, when wrinkling instability occurs in a beam, a compressive failure of the cover skin may be anticipated at a slightly higher load. The mode of failure (illustrated in fig. 2(b)) suggests, by its cylindrical deflection shape, a failure analysis based on column action of the cover. For this analysis, the cover is again idealized as shown in figure 1, except that it is restrained to buckle into a cylindrical surface. The buckling load for this idealized structure should then be tantamount to the failure load for the cover of the actual beam and readily calculated from the theory of a column deflectionally restrained by a continuous medium (see ref. 8).

The stability criterion for the cover idealized as a wide column may be written

$$k_C = \frac{\lambda^2}{b_S^2} \frac{\psi b_S^3}{\pi^4 \eta_S D_S} + \frac{b_S^2}{\lambda^2} \tag{4}$$

where the failure-stress coefficient k_C equals $\frac{\sigma_C t_S b_S^2}{\pi^2 \eta_S D_S}$, and $\frac{\psi b_S^3}{\pi^4 \eta_S D_S}$ is the channel-flange restraint parameter. (In order to include the effects of plasticity in the analysis, an effective cover flexural stiffness $\eta_S D_S$ is used in equation (4).) An expression for the channel-flange restraint parameter appropriate to an ultimate-strength analysis for the cover is given by

$$\frac{\psi b_S^3}{\pi^4 \eta_S D_S} = \frac{\frac{12}{\pi^4} \frac{\eta_W}{\eta_S}}{\left(\frac{b_W/t_W}{b_S/t_S}\right)^3 \left(\frac{f}{b_W}\right)^3} \frac{3\frac{f}{b_W} + 1}{3\frac{f}{b_W} + 4} \tag{5}$$

In equation (5), a constant value of 3 has been substituted for the parameter $\frac{\alpha b_W}{D_W}$ (see eq. (2)) which measures the continuity restraint existing between the flange and web of the channel. (Although variations in $\frac{\alpha b_W}{D_W}$ due to the influence of web stress and wave length of deformation have an effect on the initial buckling stresses for beams of various proportions, particularly when buckling tends to originate in the beam webs, the experimental data of reference 3 indicate that the stress for compressive failure of the cover is relatively unaffected by these variations. In the light of the experimental data, a value of 3 appears to be reasonable for the restraint parameter. This value corresponds to the stiffness of the web when subjected to a uniformly distributed moment along the edge joined to the flange.) With this change, equation (2) for flange stiffness becomes independent of stress and wave length.

If equation (5) is substituted into equation (4) and the failure-stress coefficient k_c is minimized with respect to wave length, the stress in the cover at failure may be expressed in the familiar form

$$\sigma_c = \frac{k_c \pi^2 \eta E}{12\left(1 - \mu^2\right)} \left(\frac{t_s}{b_s}\right)^2 \tag{6}$$

where the failure-stress coefficient is given by

$$k_c = \left[\frac{\frac{48}{\pi^4}}{\left(\frac{b_W/t_W}{b_S/t_S}\right)^3 \left(\frac{f}{b_W}\right)^3} \frac{3\frac{f}{b_W} + 1}{3\frac{f}{b_W} + 4} \right]^{\frac{1}{2}} \tag{7}$$

and

$$\eta = \sqrt{\eta_s \eta_W} \tag{8}$$

From Stowell's formulas (ref. 9), appropriate values for η_s and η_W, the plasticity coefficients for the cover skin and webs, respectively, appear to be

$$\eta_S = \frac{1}{4}\frac{E_{sec}}{E} + \frac{3}{4}\frac{E_{tan}}{E} \tag{9a}$$

$$\eta_W = \frac{E_{sec}}{E} \tag{9b}$$

which gives

$$\eta = \frac{E_{sec}}{E}\left(\frac{1}{4} + \frac{3}{4}\frac{E_{tan}}{E_{sec}}\right)^{\frac{1}{2}} \tag{10}$$

A comparison of the cover failure criterion with experimental data for beam failure is presented in figure 5. Experimental failure-stress coefficients calculated from beam failure stresses by using equation (6) are plotted for the same group of ten beams whose wrinkling-stress coefficients are plotted in figure 4. The family of curves is a plot of equation (7) for various values of $\frac{f}{b_W}$. The values of $\frac{f}{b_W}$ used in figures 4 and 5 are the same. Consideration of these two figures shows that, for beams with a known effective rivet offset distance, both failure and buckling stresses are adequately predicted by the present analysis, and that the ratio $\frac{\sigma_C}{\sigma_{cr}}$ may be as large as 1.7, although for a limited range it is essentially unity.

A broader comparison of the failure criterion with the failure-stress coefficients for the beams of reference 3 which developed a wrinkling instability is possible if an assumption is made with respect to the effective rivet offset distance for the beams. For the group of beams with $\frac{t_W}{t_S} = 0.41$, the procedure of appendix B indicated that $\frac{f}{t_W} = 7$ was applicable; the corresponding value of f is coincident with the distance between the web midplane and the near edge of the rivet shanks. The other groups of beams had somewhat different rivet diameters but had the same small ratio of rivet pitch to diameter of 3 and had the same bend radius of $4t_W$ between the attachment flange and web. Because of these similarities, it appears reasonable that the value of f for the other groups of beams may also be taken as the nominal design value of the distance between the web midplane and the near edge of the rivet shanks. The relationship between calculated and experimental failure stresses based on this approximation is shown in figure 6. The test results fall mainly within a $\pm$10-percent scatter band. Test points which fall outside the scatter band were also noted to be out of line

in the plots of failure stress given in reference 3. It appears from this figure that, as a conservative estimate for cover failure in multiweb beams for which $\frac{f}{t_W}\left(\frac{t_S}{b_S}\right) > 0.18$, a compressive stress equal to 90 percent of the value calculated from equations (6) and (7) may be used.

CONCLUDING REMARKS

Methods have been presented for correlating the wrinkling behavior of multiweb beams with the stiffness characteristics of the web members. The theory indicates that the stress for initial buckling, as well as failure, is greatly influenced by the deflectional stiffness of the web attachment flanges. Because small changes in the effective rivet offset distance f cause substantial changes in flange stiffness, the riveting specification is an important design consideration.

For evaluating attachment-flange stiffness, a procedure is suggested which has as its objective the determination of the distance from the web plane at which a given rivet pattern effectively clamps the attachment flange to the cover skin. In light of the present theory, this objective may be furthered by an analysis of existing data on compression panel strength as influenced by rivet pattern.

A comparison of test data for beams having formed-channel webs of thickness t_W with the wrinkling analysis shows satisfactory correlation. The analysis predicts that, for this type of multiweb construction, the quantity $\frac{f}{t_W}\frac{t_S}{b_S}$ must be less than about 0.18 to avoid a wrinkling instability and, hence, to achieve the buckling stresses predicted by the integral beam theory of NACA TN 1323. This criterion becomes increasingly difficult to satisfy in beams with formed-channel webs as $\frac{b_S}{t_S}$ is decreased, and the tests and theory show that the accompanying reduction in ultimate bending strength can be substantial.

Langley Aeronautical Laboratory,
National Advisory Committee for Aeronautics,
Langley Field, Va., June 2, 1954.

APPENDIX A

EVALUATION OF DEFLECTIONAL STIFFNESS FOR FORMED-CHANNEL WEBS

An expression for the deflectional stiffness of channels can be derived from a consideration of the deformation of the channel flange attached to the compression skin of the beam. At a distance f from the midplane of the channel web, the flange is considered to be completely fixed to the cover skin and to possess an elastic deflectional stiffness for small deflections. This stiffness may be evaluated by subjecting the flange to a sinusoidally distributed depthwise load of amplitude g in the presence of the appropriate longitudinal stresses in the channel.

Figure 7(a) shows the loading on the channel when wrinkling of the cover skin is initiated. The longitudinal loading is that part of the applied bending stress carried by the channel during pure bending. The sinusoidally distributed depthwise loading is applied to the flange at a distance f from the web midplane, and the ratio of this load to flange deflection is the desired deflectional stiffness ψ. Although in the beam the compressive half wave of the loading may lie closer to the web than the tensile half wave, it appears valid to assume a continuous straight-line loading when the rivet line is close to the bend radius of the channel.

The calculation of a value of ψ for given values of f, λ, and bending stress is facilitated by idealizing the channel and resolving it into component parts as shown in figure 7(b). The distortion of these parts at one cross section is illustrated in figure 7(c). The edge of the flange at $y = 0$ is assumed to be supported against deflection by the web of the channel and elastically restrained against rotation by sinusoidally distributed edge moments. The edge moments can be replaced by a rotational spring stiffness α which represents the resistance to rotation which the web offers the flange and is a function of both the wave length of deformation and the longitudinal stresses present in the web. The edge of the flange at $y = f$ is subjected to a sinusoidal depthwise load and is free to take on a deflection $w(x,f)$, but maintains a zero slope to match the wrinkling mode (case III of ref. 5) of the cover skin in a multiweb beam.

The deflected shape of the flange may be described by the function

$$w = \sin \frac{\pi x}{\lambda} \sum_{n=1,3,5}^{\infty} a_n \sin \frac{n\pi y}{2f} \tag{A1}$$

which satisfies the condition of $\frac{\partial w}{\partial y} = 0$ at $y = f$ and $w = 0$ at $y = 0$. The energy stored in the flange when it is distorted may now be written

$$U_1 = \frac{D_f}{2}\int_0^{\lambda}\int_0^{f}\left(\frac{\partial^2 w}{\partial x^2} + \frac{\partial^2 w}{\partial y^2}\right)^2 dx\,dy = \frac{D_f}{8}\pi^4\lambda f \sum_{n=1,3,5}^{\infty} a_n^2\left(\frac{1}{\lambda^2} + \frac{n^2}{4f^2}\right)^2 \tag{A2}$$

The energy stored in the rotational restraint is

$$U_2 = \frac{\alpha}{2}\int_0^{\lambda}\left(\frac{\partial w}{\partial y}\right)_{y=0}^2 dx = \frac{\alpha}{2}\int_0^{\lambda}\left(B\,\frac{\pi}{2f}\sin\frac{\pi x}{\lambda}\right)^2 dx = \frac{\alpha}{4}\left(\frac{\pi}{2f}\right)^2\lambda B^2 \tag{A3}$$

where

$$B = \sum_{n=1,3,5}^{\infty} a_n n \tag{A4}$$

The work done by the uniform load N during flange distortion is

$$V_1 = \frac{N}{2}\int_0^{\lambda}\int_0^{f}\left(\frac{\partial w}{\partial x}\right)^2 dx\,dy = \frac{N}{8}\pi^2\,\frac{f}{\lambda}\sum_{n=1,3,5}^{\infty} a_n^2 \tag{A5}$$

The work done by the sinusoidal lateral load g is

$$V_2 = \int_0^{\lambda} g\sin\frac{\pi x}{\lambda}\,w(x,f)dx = g\int_0^{\lambda} A\sin^2\frac{\pi x}{\lambda}\,dx = Ag\,\frac{\lambda}{2} \tag{A6}$$

where

$$w(x,f) = A\sin\frac{\pi x}{\lambda}$$

or

$$A = \sum_{n=1,3,5}^{\infty} a_n \sin \frac{n\pi}{2} \tag{A7}$$

The total potential energy is

$$T = U_1 + U_2 - V_1 - V_2$$

or

$$T' = \frac{8\lambda f}{\pi^4 D_f} T$$

$$= \sum_{n=1,3,5}^{\infty} a_n{}^2 \left[\left(\frac{1}{\beta} + \frac{n^2}{4} \beta \right)^2 - k_f \right] - \frac{4gf^3}{\pi^4 D_f} \beta^2 A + \frac{1}{2} \frac{\alpha f}{\pi^2 D_f} \beta^2 B^2 \tag{A8}$$

where $k_f = \frac{Nf^2}{\pi^2 D_f}$. The flange stiffness which is defined as $\psi = \frac{g}{A}$ is then found by minimizing the potential energy subject to the constraining relations in equations (A4) and (A7). The expression to be minimized is

$$Q = T' - \Delta_1 \left(\sum_{n=1,3,5}^{\infty} a_n \sin \frac{n\pi}{2} - A \right) - \Delta_2 \left(\sum_{n=1,3,5}^{\infty} a_n n - B \right) \tag{A9}$$

where Δ_1 and Δ_2 are Lagrangian multipliers. Minimization with respect to a_n, A, and B leads to the following set of equations:

$$\frac{\partial Q}{\partial a_n} = 2a_n \left[\left(\frac{1}{\beta} + \frac{n^2}{4} \beta \right)^2 - k_f \right] - \Delta_1 \sin \frac{n\pi}{2} - \Delta_2 n = 0 \tag{A10}$$

$$\frac{\partial Q}{\partial A} = -4 \frac{gf^3}{\pi^4 D_f} \beta^2 + \Delta_1 = -4A \frac{\psi f^3}{\pi^4 D_f} \beta^2 + \Delta_1 = 0 \tag{A11}$$

$$\frac{\partial Q}{\partial B} = B \frac{\alpha f}{\pi^2 D_f} \beta^2 + \Delta_2 = 0 \tag{A12}$$

which must be satisfied simultaneously with the constraining relations. Equations (A10), (A11), and (A12) may be solved for a_n, A, and B, respectively, and those expressions substituted into equations (A4) and (A7). The results are two simultaneous homogenous equations which define the flange stiffness in terms of the stresses in the web and the wave length of deformation:

$$\frac{\Delta_1}{2}\left[\sum_{n=1,3,5}^{\infty} \frac{\sin^2 \frac{n\pi}{2}}{\left(\frac{1}{\beta^2} + \frac{n^2}{4}\right)^2 - \frac{k_f}{\beta^2}} - \frac{1}{2\,\frac{\psi f^3}{\pi^4 D_f}}\right] + \frac{\Delta_2}{2} \sum_{n=1,3,5}^{\infty} \frac{n \sin \frac{n\pi}{2}}{\left(\frac{1}{\beta^2} + \frac{n^2}{4}\right)^2 - \frac{k_f}{\beta^2}} = 0 \tag{A13}$$

$$\frac{\Delta_1}{2} \sum_{n=1,3,5}^{\infty} \frac{n \sin \frac{n\pi}{2}}{\left(\frac{1}{\beta^2} + \frac{n^2}{4}\right)^2 - \frac{k_f}{\beta^2}} + \frac{\Delta_2}{2}\left[\sum_{n=1,3,5}^{\infty} \frac{n^2}{\left(\frac{1}{\beta^2} + \frac{n^2}{4}\right)^2 - \frac{k_f}{\beta^2}} + \frac{2}{\frac{\alpha f}{\pi^2 D_f}}\right] = 0 \tag{A14}$$

At this point it is worthwhile to examine the effect of simplifying the analysis by assuming that the longitudinal bending stiffness of the flange can be ignored in computing the distortion of the flange. The effect of the longitudinal bending stiffness will be small if the ratio $\beta = \frac{\lambda}{f}$ is large, as is the usual case in multiweb beams. This ratio appears in the solution as $\frac{1}{\beta^2}$, a small number, and may be set equal to zero without a serious loss in accuracy. With this simplification, equations (A13) and (A14) become

$$\frac{\Delta_1}{2}\left[\sum_{n=1,3,5}^{\infty} \frac{1}{\left(\frac{n^2}{4}\right)^2} - \frac{1}{2\,\frac{\psi f^3}{\pi^4 D_f}}\right] + \frac{\Delta_2}{2} \sum_{n=1,3,5}^{\infty} \frac{n \sin \frac{n\pi}{2}}{\left(\frac{n^2}{4}\right)^2} = 0 \tag{A15}$$

$$\frac{\Delta_1}{2}\sum_{n=1,3,5}^{\infty}\frac{n\sin\frac{n\pi}{2}}{\left(\frac{n^2}{4}\right)^2}+\frac{\Delta_2}{2}\left[\sum_{n=1,3,5}^{\infty}\frac{n^2}{\left(\frac{n^2}{4}\right)^2}+\frac{2}{\frac{\alpha f}{\pi^2 D_f}}\right]=0 \qquad (A16)$$

With the identities

$$\sum_{n=1,3,5}^{\infty}\frac{1}{n^4}\equiv\frac{\pi^4}{96}$$

$$\sum_{n=1,3,5}^{\infty}\frac{1}{n^2}\equiv\frac{\pi^2}{8}$$

$$\sum_{n=1,3,5}^{\infty}\frac{(-1)^{\frac{n-1}{2}}}{n^3}\equiv\frac{\pi^3}{32}$$

the infinite series of equations (A15) and (A16) may be written in closed form as

$$\frac{\Delta_1}{2}\left(\frac{\pi^4}{6}-\frac{1}{2\,\frac{\psi f^3}{\pi^4 D_f}}\right)+\frac{\Delta_2}{2}\frac{\pi^3}{2}=0 \qquad (A17)$$

$$\frac{\Delta_1}{2}\frac{\pi^3}{2}+\frac{\Delta_2}{2}\left(2\pi^2+\frac{2}{\frac{\alpha f}{\pi^2 D_f}}\right)=0 \qquad (A18)$$

Equations (A17) and (A18) can now be combined and solved for the deflectional restraint parameter:

$$\frac{\psi f^3}{\pi^4 D_f}=\frac{12}{\pi^4}\,\frac{\frac{\alpha f}{D_f}+1}{\frac{\alpha f}{D_f}+4} \qquad (A19)$$

When the thicknesses of the flange and the web are equal and the moduli of elasticity of webs and cover skins are equal, equation (A19) can be written

$$\frac{\psi b_S^3}{\pi^4 D_S} = \frac{\frac{12}{\pi^4}}{\left(\frac{b_W/t_W}{b_S/t_S}\right)^3 \left(\frac{f}{b_W}\right)^3} \frac{\frac{f}{b_W}\frac{\alpha b_W}{D_W} + 1}{\frac{f}{b_W}\frac{\alpha b_W}{D_W} + 4} \tag{A20}$$

Substitution of this expression into equation (A28) of reference 5 (which has been plotted in fig. 7 of ref. 5) yields the following stability criterion for multiweb beams:

$$\frac{\frac{12}{\pi^4}}{\left(\frac{b_W/t_W}{b_S/t_S}\right)^3 \left(\frac{f}{b_W}\right)^3} \frac{\frac{f}{b_W}\frac{\alpha b_W}{D_W} + 1}{\frac{f}{b_W}\frac{\alpha b_W}{D_W} + 4} = \frac{\frac{4\sqrt{k_S}}{\pi^2}\frac{\lambda}{b_S}}{\frac{\frac{\sin\varphi}{\varphi}}{1 - \cos\varphi} - \frac{\frac{\sinh\theta}{\theta}}{1 - \cosh\theta}} \tag{A21}$$

APPENDIX B

DETERMINATION OF f-DISTANCE

The method suggested herein for evaluating f (the distance between the web plane and a line along which the rivets effectively clamp the attachment flange to the cover skins) may be expected to yield valid results if the rivet pitch is small enough so that several rivets are included in each buckle length. Essentially, the method consists of experimentally measuring the stiffness of a web and its attachment flanges under a uniformly distributed depthwise loading (and when the compressive and tensile stiffnesses are not equal, calculating a substitute stiffness) and then calculating the value of f required to give this value of stiffness. The value of f so calculated is then treated as the effective rivet offset distance which can be used in equation (A20) when the web stiffness under a depthwise loading which is sinusoidally distributed along the length of the flange is being determined.

The stiffness test is carried out on a section of channel web long enough to include six or more rivets on each flange, so that a reliable average of the stiffness per unit length of channel can be obtained. The flanges of the channel are riveted to plates by using the same rivet diameter, pitch, and offset as were used in fabricating the multiweb beam, and these plates are fixed to the platens of a testing machine. Load-deflection curves are determined for the specimen under a tensile loading as well as under a compressive loading. The stiffnesses of the channel, as determined by the initial slopes of the load-deflection curves, in the two directions of loading are denoted by ψ_1 and ψ_2, where ψ_1 refers to the greater of the two stiffnesses.

Inasmuch as a single value of f is required for entering the buckling-stress curve in figure 3, it is necessary to define a single value of web stiffness ψ' to be substituted for the two measured values ψ_1 and ψ_2. The substitute stiffness ψ' is defined as the single stiffness which would absorb the same energy as a web with unequal stiffnesses ψ_1 and ψ_2 when subjected to a sinusoidally distributed deflection of unit amplitude.

The condition of equal energies of deformation is given by the following equation:

$$\frac{\psi_2}{2}\int_{a'}^{b'}\left[w(x)\right]^2 dx + \frac{\psi_1}{2}\int_{b'}^{c'}\left[w(x)\right]^2 dx = \frac{\psi'}{2}\int_{a'}^{c'}\left[w'(x)\right]^2 dx \qquad (B1)$$

in which the integration is performed over a full wave length of deformation 2λ, where $2\lambda = (b' - a') + (c' - b')$, and a', b', and c' correspond to points of zero force. Equation (B1) may be solved for the substitute stiffness with the use of the following expressions for the deflections:

$$w = a_o + \sin \frac{\pi x}{\lambda} \tag{B2}$$

$$w' = \sin \frac{\pi x}{\lambda} \tag{B3}$$

The displacement a_o in equation (B2) is determined by the condition that the deflecting forces in a full wave length must be in static equilibrium; whence,

$$\psi_2 \int_{a'}^{b'} w(x)\, dx + \psi_1 \int_{b'}^{c'} w(x)\, dx = 0 \tag{B4}$$

If equations (B2) and (B3) are substituted into equations (B1) and (B4), the following parametric equations are obtained:

$$\frac{\psi'}{\psi_2} = (1 + 2\gamma) \sin^2 \pi\gamma + \frac{3}{\pi} \sin \pi\gamma \cos \pi\gamma + \frac{1 + 2\gamma}{2} + \frac{\psi_2}{\psi_1}\left[(1 - 2\gamma) \sin^2 \pi\gamma - \frac{3}{\pi} \sin \pi\gamma \cos \pi\gamma + \frac{1 - 2\gamma}{2}\right] \tag{B5}$$

$$\frac{\psi_2}{\psi_1} = \frac{\frac{2}{\pi} \cos \pi\gamma - (1 - 2\gamma) \sin \pi\gamma}{\frac{2}{\pi} \cos \pi\gamma + (1 + 2\gamma) \sin \pi\gamma} \tag{B6}$$

where γ is defined by $a_o = \sin \pi\gamma$. A relationship between $\frac{\psi'}{\psi_2}$ and $\frac{\psi_2}{\psi_1}$ has been calculated from these equations and is plotted in figure 8. In this figure, a maximum value of ψ' equal to $3\psi_2$ is indicated when the ratio $\frac{\psi_2}{\psi_1}$ approaches zero; however, for most channel webs, the ratio $\frac{\psi'}{\psi_2}$ can be expected to be close to unity.

A value of f which would produce a value of web stiffness equal to ψ' may now be computed from the general equation for web stiffness given as equation (A19) in appendix A. In order to make this equation correspond to the loading in the channel stiffness test, the value of α is set equal to $2D_W/b_W$, the resistance of the web to a uniform distribution of edge moments which are equal but opposite in sign, and the right-hand side of equation (A19) is divided by 2 to account for the fact that, in the stiffness test, both the top and bottom flanges participate in the deflection. The resulting relation between ψ' and f when the flange and web thicknesses are the same is then given by

$$\frac{\psi' b_W^3}{D_W} = \frac{6\left(2\frac{f}{b_W} + 1\right)}{\left(\frac{f}{b_W}\right)^3\left(2\frac{f}{b_W} + 4\right)} \tag{B7}$$

A similar equation is readily derived from equation (A19) for the case in which the flanges of the channel are a different thickness from the web. For convenience in obtaining a value of $\frac{f}{b_W}$ for a given value of $\frac{\psi' b_W^3}{D_W}$, equation (B7) has been plotted in figure 9.

REFERENCES

1. Schuette, Evan H., and McCulloch, James C.: Charts for the Minimum-Weight Design of Multiweb Wings in Bending. NACA TN 1323, 1947.

2. Islinger, J. S.: Bending Tests of Multi-Web Beams Using Thick 75S-T Sheet and FS-1h Sheet Cover Skins. Rep. No. 950, ser. no. 8, McDonnell Aircraft Corp., Sept. 9, 1948, and appendix C by E. Wall, dated Mar. 16, 1951.

3. Pride, Richard A., and Anderson, Melvin S.: Experimental Investigation of the Pure-Bending Strength of 75S-T6 Aluminum-Alloy Multiweb Beams With Formed-Channel Webs. NACA TN 3082, 1954.

4. Bijlaard, P. P., and Johnston, G. S.: Compressive Buckling of Plates Due to Forced Crippling of Stiffeners. Preprint No. 408, S.M.F. Fund Paper, Inst. Aero. Sci., Jan. 1953.

5. Anderson, Roger A., and Semonian, Joseph W.: Charts Relating the Compressive Buckling Stress of Longitudinally Supported Plates to the Effective Deflectional and Rotational Stiffness of the Supports. NACA TN 2987, 1953.

6. Anderson, Roger A., Pride, Richard A., and Johnson, Aldie E., Jr.: Some Information on the Strength of Thick-Skin Wings With Multiweb and Multipost Stabilization. NACA RM L53F16, 1953.

7. Dow, Norris, F., and Hickman, William A.: Effect of Variation in Rivet Diameter and Pitch on the Average Stress at Maximum Load for 24S-T3 and 75S-T6 Aluminum-Alloy, Flat, Z-Stiffened Panels That Fail by Local Instability. NACA TN 2139, 1950.

8. Timoshenko, S.: Theory of Elastic Stability. McGraw-Hill Book Co., Inc., 1936, pp. 108-112.

9. Stowell, Elbridge Z.: A Unified Theory of Plastic Buckling of Columns and Plates. NACA Rep. 898, 1948. (Supersedes NACA TN 1556.)

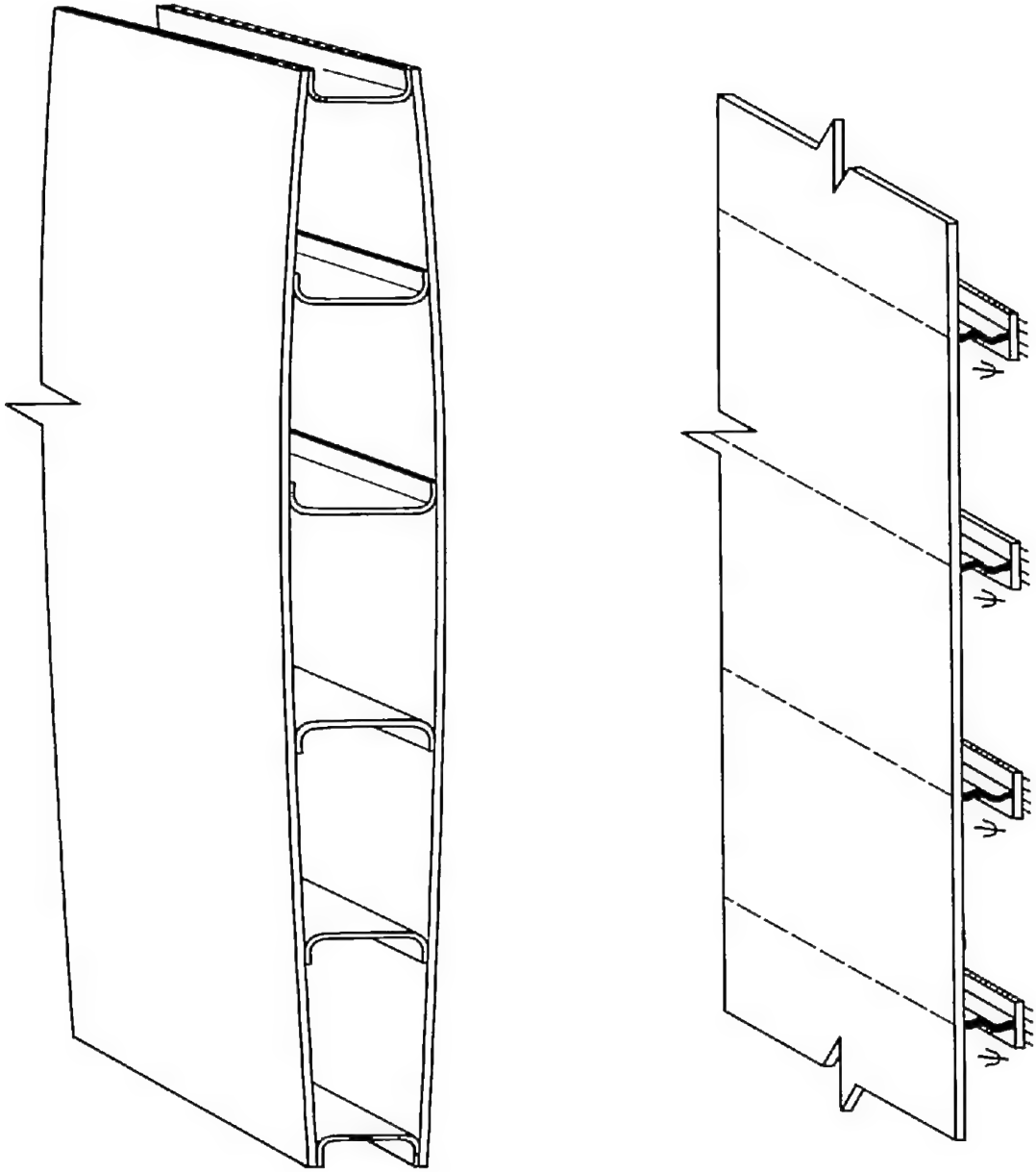

Figure 1.- Multiweb wing and structural idealization.

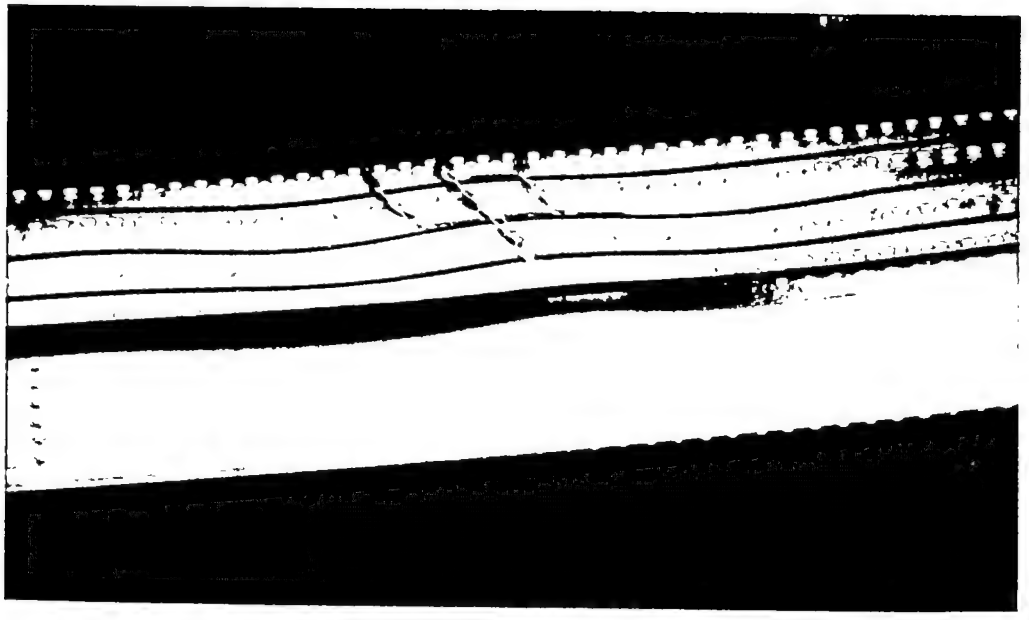

(a) Buckling.

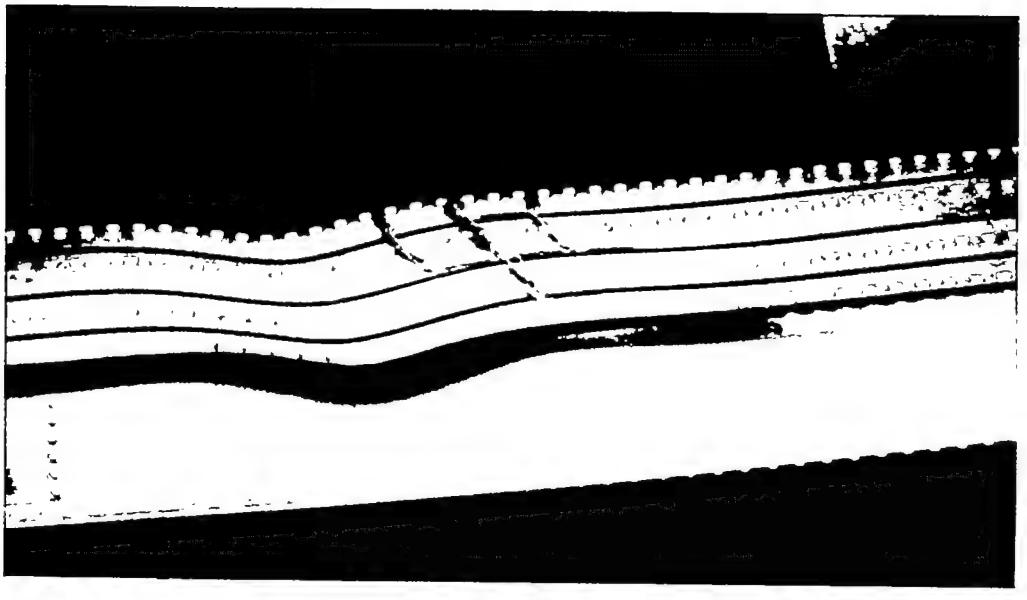

(b) Failure. L-84892

Figure 2.- Wrinkling mode of instability in multiweb beam.

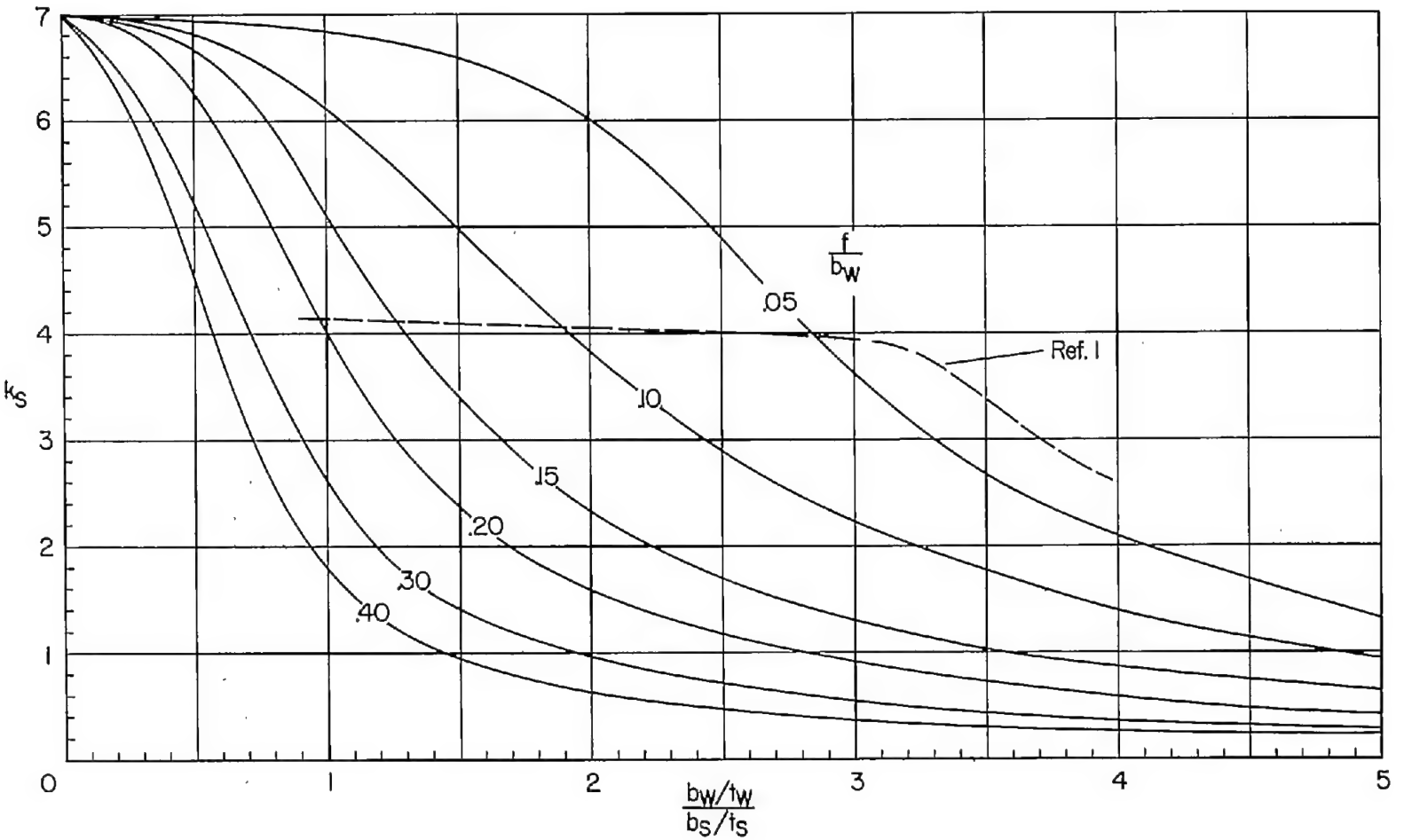

Figure 3.- Buckling curves for multiweb beams subjected to bending loads.

$$\sigma_{cr} = \frac{k_g \pi^2 E}{12(1 - \mu^2)} \left(\frac{t_s}{b_s}\right)^2 .$$

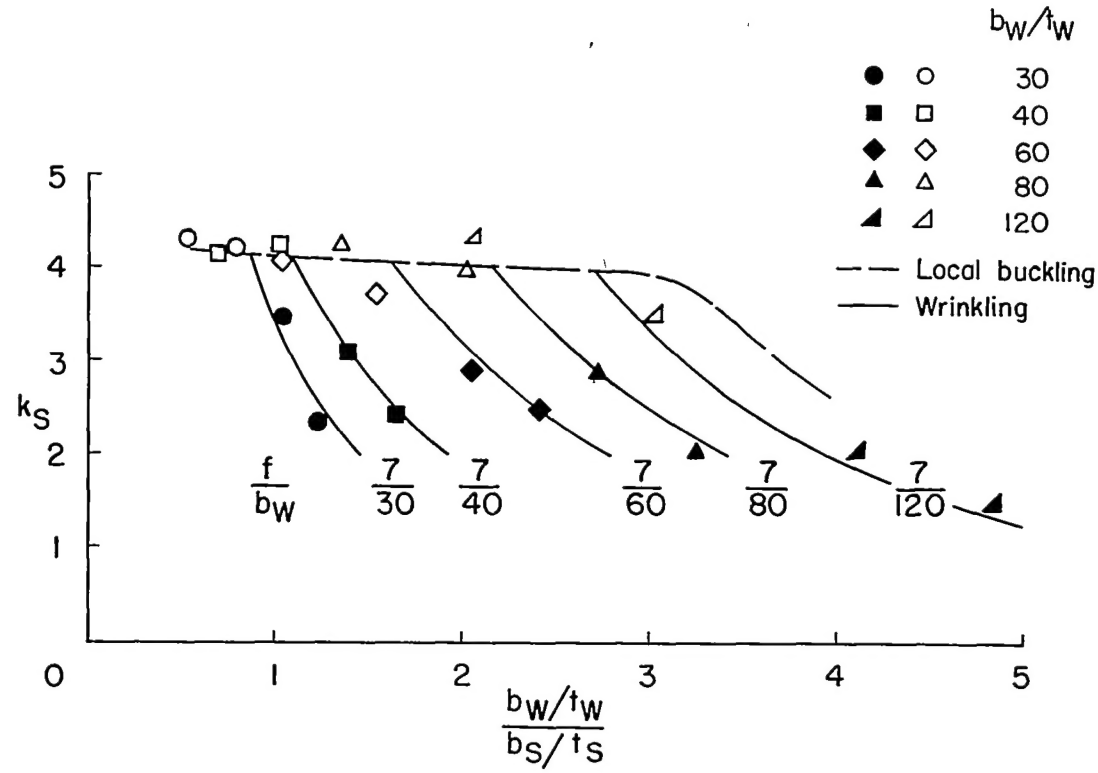

Figure 4.- Comparison of experimental buckling-stress coefficients with buckling theory. $t_W/t_S = 0.41$. Solid points represent specimens which wrinkled; open points represent specimens which buckled locally.

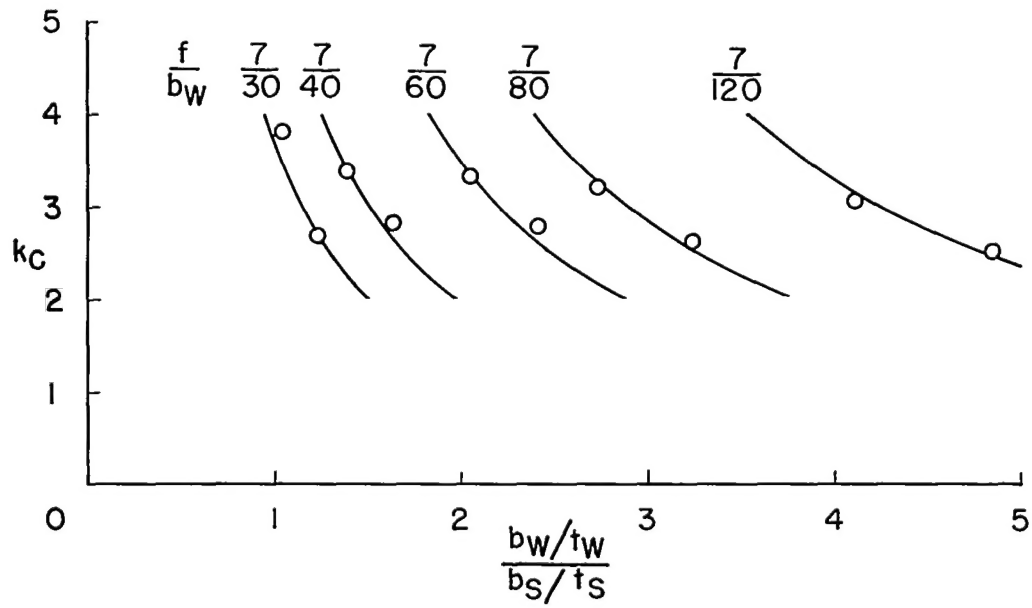

Figure 5.- Comparison of cover failure criterion with experimental data. $t_W/t_S = 0.41$; $b_S/t_S = 25, 30$; $b_W/t_W = 30, 40, 60, 80, 120$.

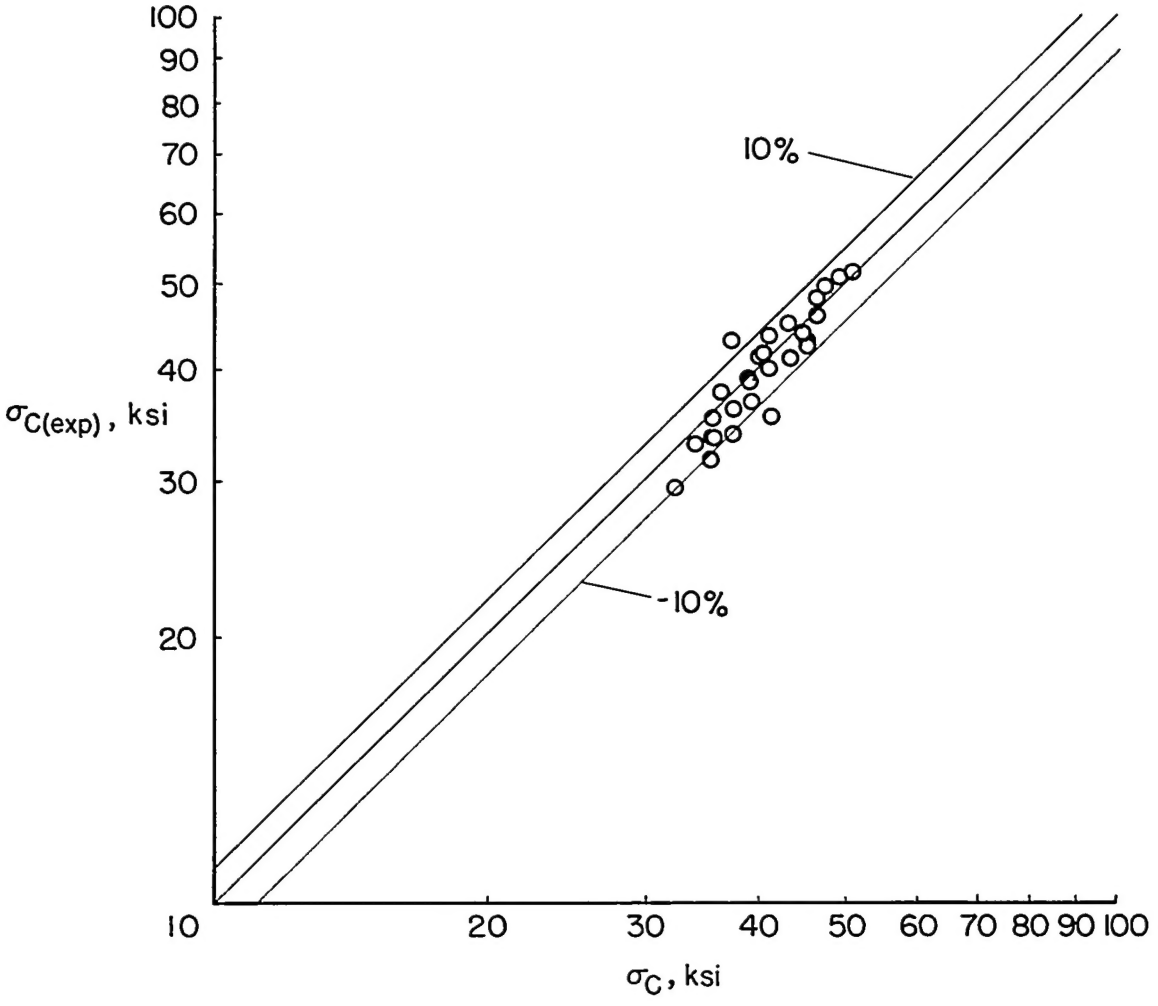

Figure 6.- Comparison of cover failure criterion with experimental failure stresses. t_W/t_S = 0.27, 0.41, 0.63; b_S/t_S = 25, 30; b_W/t_W = 30, 40, 60, 80, 120; $\sigma_C = \frac{k_C \pi^2 E}{12(1 - \mu^2)}\left(\frac{t_S}{b_S}\right)^2$.

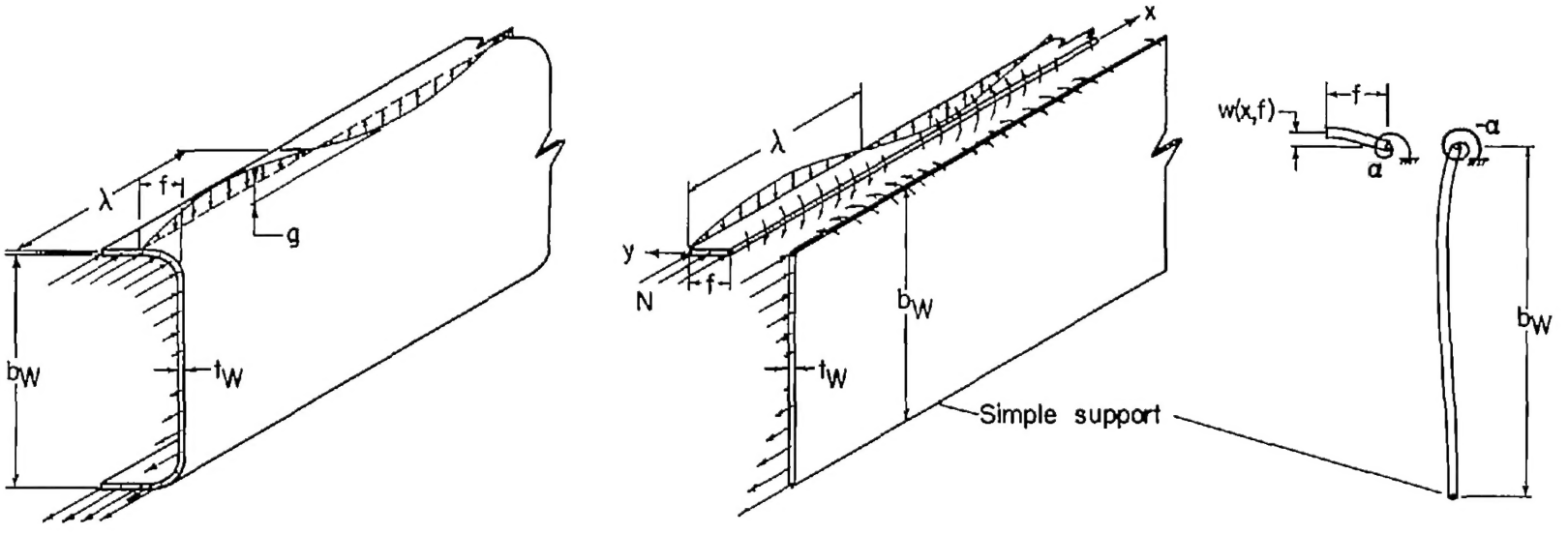

(a) Loads on channel. (b) Idealized channel. (c) Distortion of idealized channel.

Figure 7.- Loads and deformations used in calculation of effective stiffness of channel-type webs.

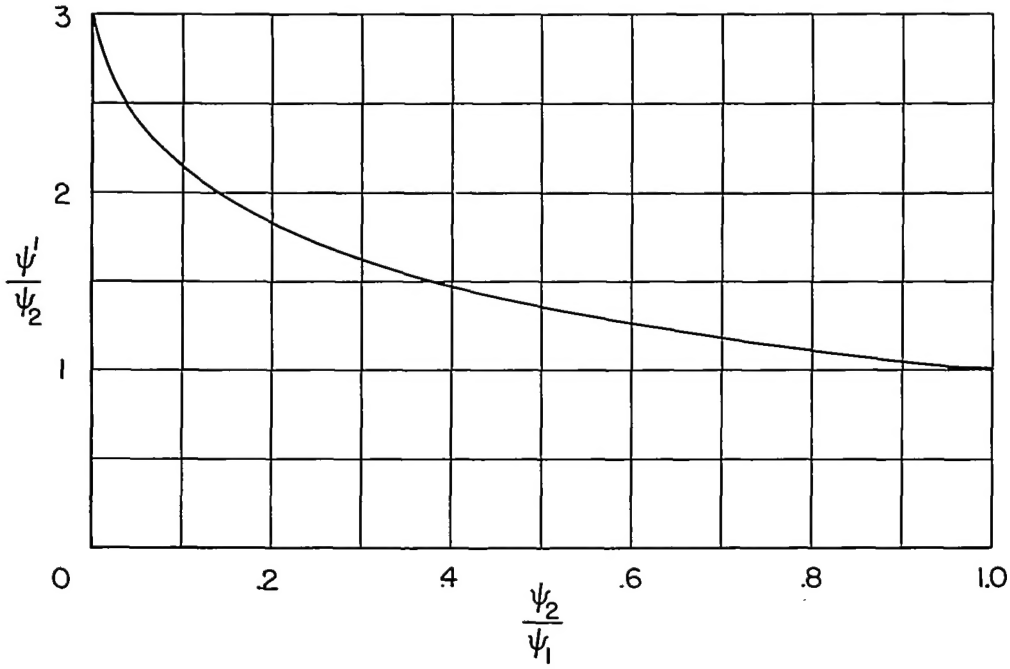

Figure 8.- Relationship between values of substitute stiffness and measured stiffness.

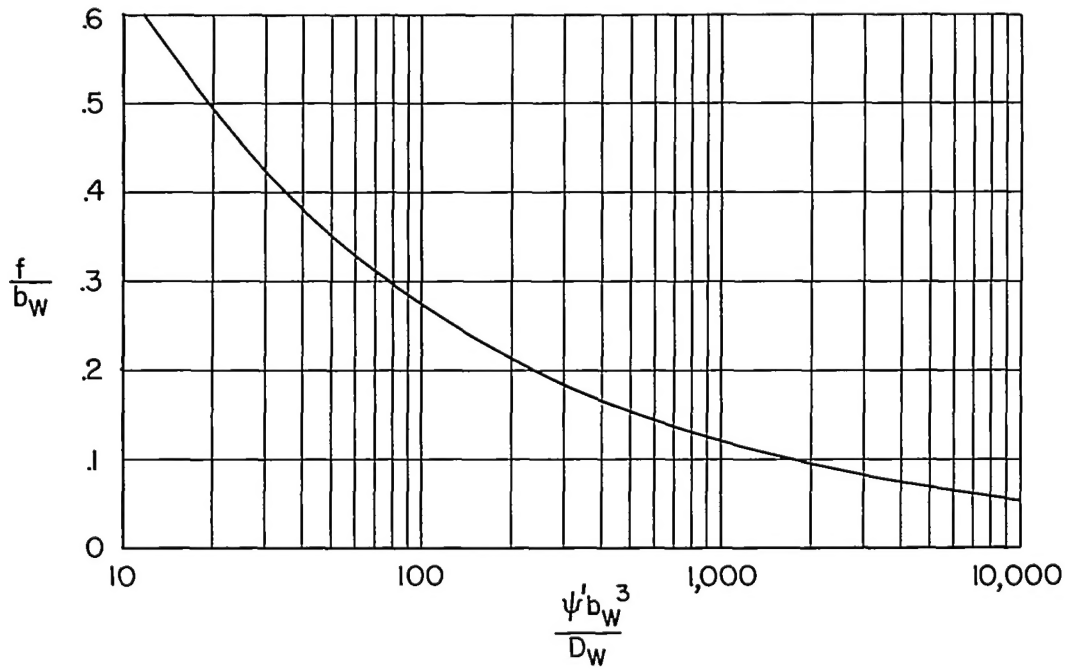

Figure 9.- Relationship between substitute stiffness and f-distance for channel-type webs.

NACA-Langley - 8-13-54 - 1000